



Synergistic Effects of Chronic Restraint-Induced Stress and Low-Dose ⁵⁶Fe-particle Irradiation on Induction of Chromosomal Aberrations in Trp53-Heterozygous Mice

| | |
|------------------------------|--|
| Author | Takanori Katsube, Bing Wang, Kaoru Tanaka, Yasuharu Ninomiya, Hirokazu Hirakawa, Cuihua Liu, Kouichi Maruyama, Guillaume Vares, Qiang Liu, Seiji Kito, Tetsuo Nakajima, Akira Fujimori, Mitsuru Neno |
| journal or publication title | Radiation Research |
| volume | 196 |
| number | 1 |
| page range | 100-112 |
| year | 2021-04-26 |
| Publisher | BioOne |
| Rights | (C)2021 by Radiation Research Society. All rights of reproduction in any form reserved. |
| Author's flag | publisher |
| URL | http://id.nii.ac.jp/1394/00002030/ |

doi: info:doi/10.1667/RADE-20-00218.1

Synergistic Effects of Chronic Restraint-Induced Stress and Low-Dose ^{56}Fe -particle Irradiation on Induction of Chromosomal Aberrations in Trp53-Heterozygous Mice

Authors: Katsube, Takanori, Wang, Bing, Tanaka, Kaoru, Ninomiya, Yasuharu, Hirakawa, Hirokazu, et al.

Source: Radiation Research, 196(1) : 100-112

Published By: Radiation Research Society

URL: <https://doi.org/10.1667/RADE-20-00218.1>

BioOne Complete (complete.BioOne.org) is a full-text database of 200 subscribed and open-access titles in the biological, ecological, and environmental sciences published by nonprofit societies, associations, museums, institutions, and presses.

Your use of this PDF, the BioOne Complete website, and all posted and associated content indicates your acceptance of BioOne's Terms of Use, available at www.bioone.org/terms-of-use.

Usage of BioOne Complete content is strictly limited to personal, educational, and non - commercial use. Commercial inquiries or rights and permissions requests should be directed to the individual publisher as copyright holder.

BioOne sees sustainable scholarly publishing as an inherently collaborative enterprise connecting authors, nonprofit publishers, academic institutions, research libraries, and research funders in the common goal of maximizing access to critical research.

Synergistic Effects of Chronic Restraint-Induced Stress and Low-Dose ⁵⁶Fe-particle Irradiation on Induction of Chromosomal Aberrations in *Trp53*-Heterozygous Mice

Takanori Katsube,^{a,1} Bing Wang,^a Kaoru Tanaka,^a Yasuharu Ninomiya,^a Hirokazu Hirakawa,^a Cuihua Liu,^a Kouichi Maruyama,^b Guillaume Vares,^c Qiang Liu,^d Seiji Kito,^e Tetsuo Nakajima,^a Akira Fujimori^a and Mitsuru Neno^{a,1}

^a National Institute of Radiological Sciences and ^b Center for Advanced Radiation Emergency Medicine, National Institutes for Quantum and Radiological Science and Technology, Chiba 263-8555, Japan; ^c Okinawa Institute of Science and Technology Graduate University, Okinawa 904-0495, Japan;

^d Institute of Radiation Medicine, Chinese Academy of Medical Sciences and Peking Union Medical College, Tianjin 300192, PR China; and ^e Center for Animal Research and Education, Nagoya University, Nagoya 464-8601, Japan

Katsube, T., Wang, B., Tanaka, K., Ninomiya, Y., Hirakawa, H., Liu, C., Maruyama, K., Vares, G., Liu, Q., Kito, S., Nakajima, T., Fujimori, A. and Neno, M. Synergistic Effects of Chronic Restraint-Induced Stress and Low-Dose ⁵⁶Fe-particle Irradiation on Induction of Chromosomal Aberrations in *Trp53*-Heterozygous Mice. *Radiat. Res.* 196, 100–112 (2021).

Astronauts can develop psychological stress (PS) during space flights due to the enclosed environment, microgravity, altered light-dark cycles, and risks of equipment failure or fatal mishaps. At the same time, they are exposed to cosmic rays including high atomic number and energy (HZE) particles such as iron-56 (Fe) ions. Psychological stress or radiation exposure can cause detrimental effects in humans. An earlier published pioneering study showed that chronic restraint-induced psychological stress (CRIPS) could attenuate *Trp53* functions and increase carcinogenesis induced by low-linear energy transfer (LET) γ rays in *Trp53*-heterozygous (*Trp53*^{+/-}) mice. To elucidate possible modification effects from CRIPS on high-LET HZE particle-induced health consequences, *Trp53*^{+/-} mice were received both CRIPS and accelerated Fe ion irradiation. Six-week-old *Trp53*^{+/-} C57BL/6N male mice were restrained 6 h per day for 28 consecutive days. On day 8, they received total-body Fe-particle irradiation (Fe-TBI, 0.1 or 2 Gy). Metaphase chromosome spreads prepared from splenocytes at the end of the 28-day restraint regimen were painted with the fluorescence *in situ* hybridization (FISH) probes for chromosomes 1 (green), 2 (red) and 3 (yellow). Induction of psychological stress in our experimental model was confirmed by increase in urinary corticosterone level on day 7 of restraint regimen. Regardless of Fe-TBI, CRIPS reduced splenocyte number per spleen at the end of the 28-day restraint regimen. At 2 Gy, Fe-TBI

alone induced many aberrant chromosomes and no modifying effect was detected from CRIPS on induction of aberrant chromosomes. Notably, neither Fe-TBI at 0.1 Gy nor CRIPS alone induced any increase in the frequency of aberrant chromosomes, while simultaneous exposure resulted in a significant increase in the frequency of chromosomal exchanges. These findings clearly showed that CRIPS could enhance the frequency of chromosomal exchanges induced by Fe-TBI at a low dose of 0.1 Gy. © 2021 by Radiation Research Society

INTRODUCTION

Outer space is comprised of ionizing radiation from cosmic rays. There are four primary radiation sources: 1. Galactic cosmic rays (GCRs) come from outside the solar system; 2. Chronic low-dose-rate ejections of solar energetic particles (SEPs) from the sun in steady state; 3. Short-term emissions of higher-dose-rate SEP or solar particle events (SPEs) originating from the sun; and 4. Energetic electrons and protons trapped in the Van Allen Belts around the earth (1–3). Among them, the steady-state chronic low-dose-rate SEPs pose little health hazard since they consist mainly of protons and electrons with very low energies and will be stopped within aluminum or plastic shielding materials (2, 3). SPEs are grouped into two classes. The smaller events, termed impulsive events or impulsive flares, are short-lived, usually of the order of hours. The larger events, referred to as gradual events or coronal mass ejections (CMEs), are much longer-lived, of the order of days. GCRs and SPEs are mostly constituted from high-energy charged particles including electrons, protons (nucleus of hydrogen), alpha particles (nucleus of helium) and nuclei of other elements larger than helium called high atomic number and energy (HZE) particles (1–3). On Earth, we are well protected from cosmic rays by the magnetic field and atmosphere. Exposure to cosmic rays is one of the major health concerns

¹ Address for correspondence: Dr. Takanori Katsube, National Institute of Radiological Sciences, National Institutes for Quantum and Radiological Science and Technology, 4-9-1, Anagawa, Inage-ku, Chiba 263-8555, Japan; email: katsube.takanori@qst.go.jp; and Dr. Mitsuru Neno, National Institute of Radiological Sciences, National Institutes for Quantum and Radiological Science and Technology, 4-9-1, Anagawa, Inage-ku, Chiba 263-8555, Japan; email: neno.mitsuru@qst.go.jp.

for spaceflight crews (4, 5). Currently, most manned space missions are destined to space stations such as the International Space Station (ISS) in low-Earth orbits, where spaceflight crews are somewhat protected from cosmic rays by the magnetic field of the Earth (6). Because there is neither a protective magnetic field on the moon and Mars, nor in interplanetary space, spaceflight crews will be exposed to GCRs and SPEs, including HZE particles, on the future missions to lunar and Mars orbit and surface at higher dose rate and for longer duration than most crews onboard space stations in low-Earth orbit (3, 4).

GCRs consist of 86.3% low-linear energy transfer (LET) protons, 12.8% helium ions and remaining 0.9% HZE particles (2, 7, 8). HZE particles are often referred to as densely ionizing or high-LET radiation as they deposit a large amount of energy along their trajectory and result in a high ionization density along the center of the particle path (9). High-LET radiations generally have greater potential for causing DNA damage and show higher biological effectiveness than low-LET radiations such as gamma (γ) or X rays. While HZE particles make up only 0.9% of GCRs, they will make up 88.1% of the estimated ionizing dose equivalent from GCR exposure during deep space travel and contribute significantly to the overall biological effects of cosmic rays (2, 7, 8).

Up to now, more than 559 humans have been to outer space, mostly within low-Earth orbit (10). The longest is the 438-day mission at the space station Mir completed by cosmonaut Valeri V. Polyakov in March 1995 (6). ISS hosted 170 long-duration crewmember flights, ranging from 48 to 340 days, until March 2020. The majority of the flights were five to seven months long (6). During spaceflight, crews frequently develop psychological stress (PS) because of enclosed environment, microgravity, altered light-dark cycles, and risks of equipment failure or fatal mishaps. According to conceptual design studies of NASA, the future missions to Mars may take 800–1,000 days, of which approximately 500 days will be spent on the surface of the planet (11). Such long-term confinement to a spacecraft and isolation from the earth will increase the risk for Mars mission crews to develop a much higher level of psychological stress than any previous space crews.

Based on the findings of epidemiological studies, psychological stress has been suggested to increase the risk of various conditions, such as vision disorders, hypertension, cardiovascular diseases, diabetes, metabolic syndrome, Alzheimer's disease and cancer development (12–18). The dysregulation of the immune and other body systems mediated by the hypothalamic-pituitary-adrenal (HPA) axis and sympatho-adreno-medullary (SAM) system in response to psychological stress is the main pathophysiological process underlying the detrimental health consequences of psychological stress (19–22). Multiple published studies have shown that most spaceflight crews present with reductions in T-cell function, NK

cell function, elevated plasma cytokine profiles and persistent inflammation while in outer space (23–26). Therefore, not only psychological stress but also immune system weakening are considered to be major health concerns for spaceflight crews (27, 28).

Accumulating evidence suggests that psychological stress alone cannot cause cancer but that inflammation and dysregulation of immune systems resulting from psychological stress accelerate promotion, progression and metastasis of existing premalignant cells (12, 19, 21, 29). It is well established that ionizing radiation induces DNA damages, which can lead to genetic mutations and cell death and also contribute to the initiation and promotion of carcinogenesis (30). Feng *et al.* showed that chronic restraint-induced psychological stress (CRIPS) promoted radiocarcinogenesis induced by γ rays using *Trp53*-heterozygous (*Trp53*^{+/-}) C57BL/6J mice (31). In previously reported work, we demonstrated modulatory effects of CRIPS on the frequency of chromosomal aberrations (CAs) induced by X rays in splenocytes of *Trp53*-wild-type (*Trp53*^{+/+}) C57BL/6J mice (32). The goal of our current study is to elucidate the possible consequences of exposure to both psychological stress and HZE particles on astronauts using an animal model. We here utilized a CRIPS model of *Trp53*-heterozygous (*Trp53*^{+/-}) C57BL/6N mice, a sensitive model to detect radiation-induced tumorigenic process, and focused especially on the genotoxic effects from Fe ions, the most densely ionizing particles present in a relatively large amount in GCRs.

MATERIALS AND METHODS

Animals and Experimental Design

Trp53-heterozygous (*Trp53*^{+/-}) C57BL/6N male mice (BRC NO. 01361, CDB 0001K) (33) were bred and maintained in a clean conventional animal facility at the National Institute of Radiological Sciences (NIRS, QST, Chiba, Japan) under a 12:12 h light-dark schedule (lights on from 7:00 a.m. to 7:00 p.m.) and controlled temperature (23 \pm 2°C) and humidity (50 \pm 10%). Animals housed in autoclaved cages (1–2 mice per cage) with sterilized wood chips were allowed free access to standard laboratory chow (MB-1; Funabashi Farm Co., Japan) and acidified water (pH 3.0 \pm 0.2). Animals were acclimatized to the laboratory conditions for 2 weeks before use. Six-week-old mice were randomly assigned to six experimental groups with 6–7 mice in each group: The “free and 0.0 Gy group (F00)”, receiving neither restraint nor total-body irradiation with ⁵⁶Fe-particles (Fe-TBI); the “free and 0.1 Gy group (F01)”, receiving only Fe-TBI at 0.1 Gy; the “free and 2.0 Gy group (F20)”, receiving only 2.0 Gy Fe-TBI; the “restraint and 0.0 Gy group (R00)”, receiving only chronic restraint; the “restraint and 0.1 Gy group (R01)”, receiving chronic restraint and 0.1 Gy Fe-TBI; and the “restraint and 2.0 Gy group (R20)”, receiving chronic restraint and 2.0 Gy Fe-TBI. Chronic restraint, a well-established typical mouse model to induce psychological stress (31), was applied to mice as described elsewhere (34). In brief, the mouse restraint system (Flat Bottom Rodent Holder, Kent Scientific Corp., Torrington, CT) was used for chronic periodic restraint on a daily basis of 6 h for 28 consecutive days. Individual 6-week-old mice were placed in the restrainer and maintained horizontally in their home cage during the 6-h restraint session (9:30 a.m. to 3:30 p.m.) daily. Animals were

then released into the same cage and allowed access to food and water during the free session (3:30 p.m. to 9:30 a.m.). The F00, F01 and F20 groups received no restraint, but food and water were withheld at the same time as for the R00, R01 and R20 groups during the 6-h restraint session each day. Fe-TBI was performed using a Heavy Ion Medical Accelerator in Chiba (HIMAC) at NIRS-QST. ^{56}Fe -particles (500 MeV/u) of 0.1 or 2.0 Gy were delivered at a dose rate of 0.08–0.09 or 1.0–2.0 Gy/min, respectively, to the F01, R01, F20 and R20 groups in the early morning (3:30–04:30 a.m. or 6:00–7:00 a.m.) on day 8 of the 28-day restraint regimen. The dose-averaged LET value of Fe-particles calculated by Monte Carlo simulation was $200 \pm 20 \text{ KeV}/\mu\text{m}$. Three mice held in an acrylic cylinder container with three individual cells of the same size (each mouse in each cell) received Fe-TBI at room temperature without anesthesia. The mice were in an air-breathing condition (there were six holes 5 mm in diameter in the wall of each cell) during irradiation. One or two male mice that were from the same dam and had been together since birth, were housed in a cage during the 28-day restraint regimen. No fighting was observed among mice in any of the cages. All experimental protocols involving mice were reviewed and approved by the Institutional Animal Care and Use Committee of NIRS. Experiments were performed in strict accordance with NIRS Guidelines for the Care and Use of Laboratory Animals.

Measurements of Urinary Corticosterone

Urine samples from mice were collected in the morning on day 7 of the 28-day restraint regimen. Concentrations of urinary corticosterone in the samples were determined using the AssayMax Corticosterone ELISA kit (Assaypro, St. Charles, MO) according to the manufacturer's protocol.

Isolation of Splenocytes and Determination of Splenocyte Numbers

At the end of the 28-day restraint regimen, mice were anesthetized by inhalation of gaseous isoflurane (2-chloro-2-(difluoromethoxy)-1,1,1-trifluoro-ethane) (Sigma-Aldrich, Japan) and then euthanized by cervical dislocation. Spleens were removed aseptically. Splenocytes were isolated by gently pressing the spleen tissue with the plunger end of a 1-ml syringe on a cell strainer (Corning® Inc., Corning, NY) and washing out the cells with RPMI 1640 medium (Sigma-Aldrich) supplemented with 10% fetal bovine serum (JRH Biosciences, Lenexa, KS), 100 U/ml penicillin G, 100 mg/ml streptomycin (Sigma-Aldrich), 10 mg/ml lipopolysaccharide (Sigma-Aldrich, Japan), 3 mg/ml concanavalin A (Sigma-Aldrich), and 50 mM 2-mercaptoethanol (Wako, Japan). To determine the number of splenocytes per spleen, cells were counted using a hemocytometer. (Red blood cells with a small diameter were omitted from the cell count.)

Preparation of Chromosomes from Splenocytes

Splenocytes were cultured in the same media described above (5×10^6 cells/5 ml) at 37°C in a humidified 5% CO₂ atmosphere for 24 h. Colcemid (0.1 mg/ml, KaryoMAX®, Life Technologies, Grand Island, NY) was added to the last 2 h of the culture. Cells were harvested, swollen in 75 mM KCl at room temperature for 12 min, and then fixed with the standard methanol-acetic acid fixative (3:1). After 2–3 additional changes of fixative, the cell suspension was dropped onto a wet, clean slide to obtain chromosome spreads. This protocol ensured that virtually most metaphase cells observed were in their first mitotic division under the *in vitro* culture.

Fluorescence in situ Hybridization (FISH)

Air-dried slide preparations with chromosome spreads were incubated at 62–65°C for 2 h and then treated with 0.2 N HCl at

room temperature for 1 h. The slides were painted with FISH probes for chromosomes 1, 2 and 3 (XMP 1 green, XMP 2 orange, XMP 3 green, and XMP 3 orange; XCYting Mouse Chromosome Painting Probes; MetaSystems, Germany) according to the manufacturer's instructions. In brief, probes were applied to the slides, denatured at 75°C for 2 min, and then incubated at 37°C overnight. The slides were washed and counterstained with DAPI in antifade reagent (MetaSystems). Chromosomes 1, 2 and 3 represent 7.0%, 6.5% and 5.7% of the genome, respectively. When these probes are hybridized simultaneously, it is possible to detect 33% of all inter-chromosome exchanges (32). Thus, when one CA is found in 100 cells, the frequency of CAs occurring in the whole genome can be estimated as $3 (=1/0.33)$ per 100 cell equivalent.

Scoring of CAs

Metaphase cells were analyzed using an automatic slide scanning system consisting of a motorized microscope (Axio Imager Z2; Carl Zeiss, Germany), digital CCD camera (CoolCube 1m; MetaSystems), and the image analysis program Metafer 4 with an MSearch module (MetaSystems). After automated metaphase cell finding, digitalized high-resolution images were captured automatically at 100× magnification. Metaphase cells were considered scoreable if they met the following criteria: 1. The cells appeared to be intact; 2. The centromeres of the chromosomes were readily identifiable; 3. The centromeres of all the painted chromosomes were present; and 4. The hybridization label was sufficiently bright to detect exchanges between painted and unpainted chromosomes. Chromosomal exchanges involving chromosome 1, 2 or 3 were identified as color junctions (CJs) within a chromosome and were scored according to the PAINT system (35). Aberrant chromosomes were classified as translocations, insertions, dicentric (DCs) and acentric fragments (AFs). Monocentric chromosomes with CJs were scored as translocations even if those had multiple CJs. However, when monocentric chromosomes possessed two junctions such that the flanking pieces were the same color, the chromosomes were classified as insertions and excluded from the total for translocations. Robertsonian translocations or centric fusions were not scored because they display some different features from other common translocations, including relatively high spontaneous incidence and non-random occurrence, probably ascribed to satellite sequences in centromeric area (36, 37). DCs were identified as the chromosomes with two centromeres at both ends, while only DCs with at least one CJ were scored in the PAINT system, here we scored DCs without color junctions as well. Chromosomal fragments without centromeres were scored as AFs when they had CJs or when they were painted whole length with one FISH probe. Former ones might result from chromosomal exchanging events producing DCs with CJs, and later ones from unrepaired chromosomal breaks of chromosome 1, 2 or 3. Chromosomes with more than two centromeres were not found here due to the acrocentric morphology of mouse chromosomes. At least 200 metaphase cells were scored for each mouse in general and more than 400 metaphase cells were scored for the mouse in which abnormal cells accounted for less than 1%. All slides were coded prior to scoring and observed by at least two investigators independently to minimize observer bias. Here, abnormal cells are the cells with any aberrant chromosomes scored as above.

Statistical Analysis

Statistical differences between means \pm standard deviations from two groups were evaluated using Student's *t* test or Welch's unequal variances *t* test after the *F* test of equality of variances. Significance was assigned to $P < 0.05$. Because the current study involves exploratory research on radiation risk, *b* error, including overlooking risk, is more harmful than a error, and there is no point in keeping a error at a strictly nominal level. Therefore, no a adjustment for multiple testing was conducted (38).

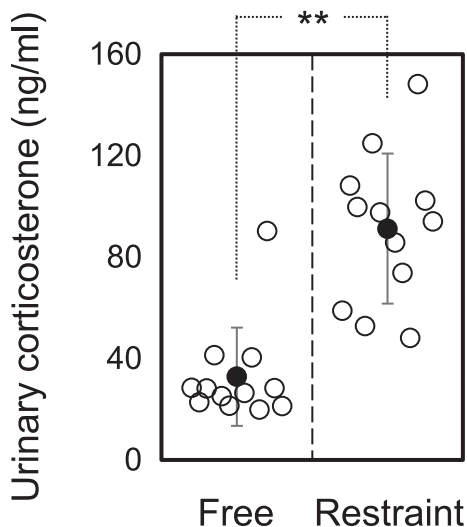


FIG. 1. Induction of urinary corticosterone by chronic restraint. Concentrations of corticosterone in mouse urine obtained on the morning of day 7 of consecutive restraint regimen were measured. Open circles indicate the values for individual mice and closed circles with vertical bars indicate the mean values with standard deviations of each group. Statistically significant difference indicated at $**P < 0.001$.

RESULTS

CRIPS Reduced the Splenocyte Number per Spleen

To determine whether psychological stress influences the biological effects induced by high-LET radiation, we utilized a well-established typical mouse model, in which chronic physical restraint was applied to mice to induce psychological stress. Six-week-old male *Trp53^{+/-}* C57BL/6N mice were immobilized in a mouse restraint apparatus 6 h/day (9:30 a.m. to 3:30 p.m.) for 28 consecutive days and received Fe-TBI at 0.0, 0.1 or 2.0 Gy in the early morning (before the start of a 6-h restraint session at 9:30 a.m.) of day 8. To verify a successful induction of psychological stress by chronic restraint, urine samples were collected from 12 restraint and 12 non-immobilized free mice just before the start of 6-h restraint session on day 7, and the concentrations of corticosterone, a stress hormone, in the urine samples were determined (Fig. 1). All of the 12 restrained mice showed higher urinary corticosterone levels than 11 of the 12 free mice. The difference between the average levels for the 12 restrained and the 12 free mice was statistically significant. On the first day after the 28-day restraint regimen, splenocytes were isolated for chromosome analysis. No lethality due to hematopoietic syndrome or GI damage was induced after 2 Gy Fe-TBI. Figure 2 shows the splenocyte number per spleen of each mice. Only CRIPS had a significant effect on the splenocyte number per spleen. There were significant statistical differences in every comparison between non-immobilized free groups (F00, F01 and F20) and restrained groups (R00, R01 and R20). On the other hand, within the non-immobilized free groups

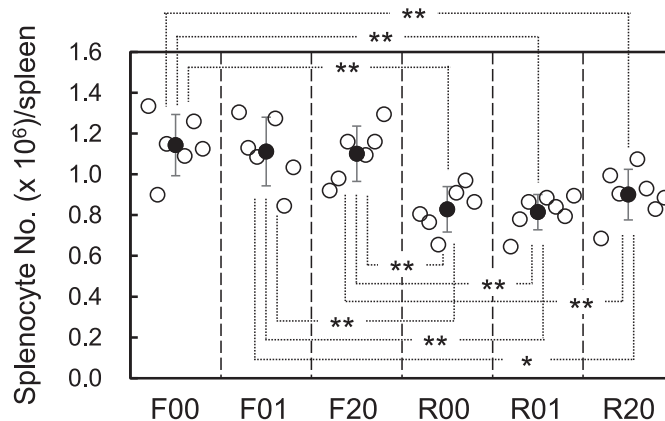


FIG. 2. Effects of CRIPS and Fe-TBI on splenocyte numbers per spleen. Open circles indicate the values for individual mice of each group: Free + 0.0 Gy group (F00); free + 0.1 Gy (F01); free + 2.0 Gy (F20); restraint + 0.0 Gy (R00); restraint + 0.1 Gy (R01); and restraint + 2.0 Gy (R20). Closed symbols with vertical bars indicate the mean numbers with standard deviations of each group. Statistically significant differences are indicated at $*P < 0.05$ and $**P < 0.001$.

or the restrained groups, no significant difference was observed regardless of radiation dose (0, 0.1 or 2.0 Gy).

Effects of CRIPS on CAs Induced by Fe-TBI

Metaphase chromosomes were prepared from splenocytes, visualized using FISH probes specific to chromosomes 1, 2 and 3, and counterstained with DAPI. Aberrant chromosomes involving FISH paintings were scored according to the modified PAINT system as described in Materials and Methods and the results are summarized in Tables 1 and 2. While only DCs involving FISH paintings were scored in the PAINT system, we also scored DCs without FISH paintings and showed the total frequency of DCs with and without FISH paintings as “whole DCs” in Table 1.

We observed a total of 14,340 metaphase cells of 38 mice from six experimental groups and found 149 abnormal cells, among which 100 cells had at least one aberrant chromosome with CJs and the remaining 49 cells had only aberrant chromosomes without CJs, such as FISH painted AFs, probably from unrepaired chromosomal breaks of chromosomes 1, 2 and 3 or DCs without FISH paintings. Among the 100 cells with CJs, 83 (83%) had an even number (2 or 4) of the CJs. Figure 3 shows the distribution of the color junction number per cell of each experimental group. The cells with two CJs were most abundant in every group. These results suggested that most of the abnormal cells contained apparently simple exchanges, i.e., either reciprocal translocations or DCs with paired AFs at the observed time point.

Table 2 summarizes the distribution of the number of CJs in an aberrant chromosome. We found 201 aberrant chromosomes with CJs in 100 abnormal cells. Among the 201 aberrant chromosomes, 178 (88.6%) contained only one CJ and might have resulted from simple exchanges, i.e.,

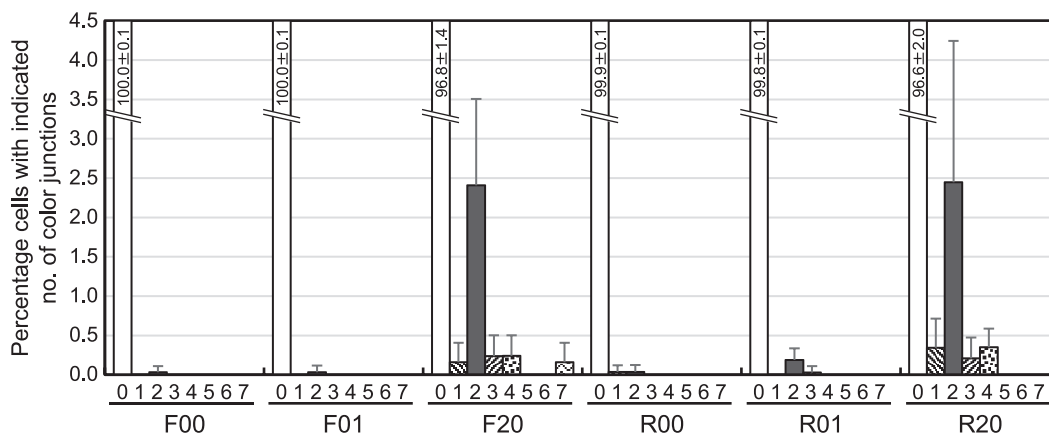


FIG. 3. The distribution of color junctions by cell from mice subjected to CRIPS and/or Fe-TBI. The percentage of cells with the indicated number of color junctions within each mouse was determined and the average values of 6 or 7 mice were shown with standard errors. All the average values for cells without color junctions exceeded 95% and are shown within each bar.

either reciprocal translocations or DCs associating with AFs. Those 178 CAs were 134 translocations, 23 DCs and 21 AFs. The remaining 23 (11.4%) aberrant chromosomes contained multiple CJs; these were two chromosomes harboring two translocations, 16 chromosomes with an insertion, two DCs with two CJs and three AFs with two or three CJs. It is noteworthy that while most (21/23) of the aberrant chromosomes harboring multiple CJs were found in the experimental groups that received high-dose Fe-TBI (F20 and R20), two were found in the CRIPS plus low-dose Fe-TBI (R01) group and none were found in other groups receiving low-dose Fe-TBI alone (F01) or no Fe-TBI (F00 and R00).

As shown in Table 1, metaphase cells with aberrant chromosomes (abnormal cells) accounted for over 4.5% on average of observed cells in the high-dose Fe-TBI groups (F20 and R20) but less than 0.4 % on average in other groups with low-dose or no Fe-TBI (F00, F01, R00 and R01). The frequencies of abnormal cells, CJs, stable-type CAs, unstable-type CAs and whole DCs are shown graphically in Fig. 4. In every class, the frequencies in high-dose Fe-TBI groups (F20 and R20) were significantly higher than those in each of other groups (F00, F01, R00 and R01), while there were no significant differences between the F20 and R20 groups. We could not find any statistically significant differences among four low-dose or 0 Gy Fe-TBI groups in every class of aberrations except in the frequencies of CJs. CJs were found in 6 of 7 mice in R01, and in 1 or 2 out of 6 in other groups, F00, F01 and R00. Statistical analysis showed that the average value of CJ frequency in the R01 group was significantly higher than those in F00, F01 and R00. These results suggest that concurrent exposure to CRIPS and low-dose Fe-TBI could induce chromosomal exchanges significantly but neither CRIPS nor low-dose Fe-TBI alone.

DISCUSSION

Both exposure to cosmic rays and development of psychological stress from challenging space environments, such as confinement to a spacecraft, isolation from the earth, microgravity and risks of equipment failure or fatal mishaps, are of major health concern for spaceflight crews, especially in the case of future lunar or Mars missions (27, 28, 39, 40). The goal of this study was to elucidate the possible combined effect of exposure to both cosmic rays and psychological stress. In particular, we focused on Fe-TBI and its genotoxic effects in mice under psychological stress. Fe ion particles have received much attention, because they are the most densely ionizing particles present in relatively large amounts in GCRs (3).

Chronic restraint is a well-established typical mouse model to induce psychological stress (31). Animals treated with our restraint protocol showed several features commonly observed in CRIPS models, such as significant decreases in body weight gain and in the weights of immune organs, such as the thymus and spleen (data not shown). In addition, an increase in urinary corticosterone levels was demonstrated in these mice after seven consecutive days of chronic restraint (6 h per day) (Fig. 1). These results confirmed that our experimental model reproduces CRIPS.

Observation at the end of the 4-week restraint regimen revealed that CRIPS alone resulted in 27% reduction in average number of splenocytes per spleen, while Fe-TBI on day 8 did not induce any significant effects by itself on splenocyte number even at high dose (2.0 Gy), nor any additional effects in combination with CRIPS (Fig. 2). On the other hand, our previously published work using *Trp53^{+/+}* C57BL/6J mice showed that either CRIPS or 4 Gy total-body X-ray irradiation resulted in reduction in splenocyte number by 53% or 20% at the end of a 4-week restraint regimen, respectively (32). In addition, in a

published study by Gridley *et al.*, analysis was performed on the effects of Fe-TBI at doses from 0.1 Gy to 3.0 Gy on immune cells of C57BL/6J mice and showed that Fe-TBI generally decreased splenic lymphocyte counts with increasing dose. This response was most pronounced on day 4 after TBI and while reduced over subsequent days, it was still not entirely absent by day 30 (41, 42). A comparison of these observations indicates that the effects of CRIPS as well as ionizing radiation may be underexpressed in *Trp53*^{+/-} (C57BL/6N) mice compared to *Trp53*^{+/+} (C57BL/6J) mice. Because *Trp53* is a key regulator of cell cycle progression and apoptosis, among possible reasons, haploinsufficiency of *Trp53* gene may be a cause for different response in splenocyte number to CRIPS and ionizing radiation between *Trp53*^{+/-} and *Trp53*^{+/+} mice.

To gain insight into the influence of CRIPS on the genotoxic effects of Fe-TBI, we evaluated induction of aberrant chromosomes in the splenocytes of *Trp53*^{+/-} mice that concomitantly underwent CRIPS and Fe-TBI (0.0, 0.1 and 2.0 Gy) by FISH painting of chromosomes 1, 2 and 3. In the current work, no mice died during experiment. The latitude of the higher dose (2.0 Gy) used was much lower than the documented lethal dose of 5.8 Gy, which has caused 50% lethality within 30 day (43). Fe-TBI at 2 Gy yielded many aberrant chromosomes. The average values of the frequencies of abnormal cells, CJs, stable-type CAs, unstable-type CAs and whole DCs (including DCs without CJs) in 2 Gy Fe-TBI groups (F20 and R20) were significantly higher than those in the 0 and 0.1 Gy Fe-TBI groups (F00, F01, R00 and R01) (Fig. 4). However, we could not find any statistically significant differences in average values of the frequencies between the F20 and R20 groups. If CRIPS has some modifying effects on induction of CAs after Fe-TBI, they are most likely too small to be detected with 2 Gy Fe-TBI, by which CAs were induced at high frequency with relatively large variations among individual mice.

When the comparisons were made among 0 Gy and low-dose Fe-TBI groups (F00, F01, R00 and R01), it appeared that neither CRIPS nor 0.1 Gy Fe-TBI could increase any kind of aberrant chromosomes but concomitant exposure could increase CJs in the splenocytes of *Trp53*^{+/-} mice at least at 3 weeks after TBI. Here, CJs correspond to the number of loci where chromosomal exchanges have occurred. On the other hand, CAs represent the number of chromosomes containing some chromosomal exchanges or breaks. When multiple exchanging events have occurred in a chromosome, we score every event as a CJ but only once as a CA. Aberrant cells represent cells with any CAs and a cell harboring multiple CAs is counted only once. Generally, high-LET radiation yields complex aberrations defined as chromosome exchanges involving at least three breaks in two or more chromosomes more frequently than low-LET radiation (44, 45). Therefore, scoring of CJs should be the most sensitive way to detect the difference in the frequency of chromosomal exchange

events. Stable-type CAs were found in 4 of 7 mice in the R01 group, and zero or one of 6 mice in F00, F01 and R00 groups (Table 1 and Fig. 4). Probably due to the insufficient number of metaphase cells observed, a small increase of stable-type CAs was not detected in R01 compared to the F00, F01 and R00 groups in the statistical analysis. In addition, here AFs include those without CJs from unrepaired chromosomal breaks of chromosomes 1, 2 and 3. Basal level of such AFs without CJs was relatively high and may have disturbed the detection of a relatively small-combined effect of CRIPS and low-dose Fe-TBI on inducing unstable-type CAs as well as abnormal cells.

Generally, chromosomal exchanges have been attributed to the generation of multiple double-strand breaks (DSBs) and following mis-rejoining of them. Two assumptions can be proposed to explain how CRIPS and 0.1 Gy Fe-TBI synergize to induce chromosomal exchanges. The first is the increase in the yield of DNA damages and/or chromosomal exchanges themselves and the second is the reduced removal of aberrant chromosomes. The first assumption may be achieved by the activation of the reactive oxygen species (ROS) generating system by CRIPS, leading to an increase in DSBs. It was documented in animal models that psychological stress increased the production of oxidative DNA damage, CAs and sister chromatid exchanges (SCEs) (46, 47). In human studies, positive relationships were found between superoxide production and the stress of taking an examination and between 8-hydroxy-2'-deoxyguanosine (8-OHdG) levels and various psychological factors, including anxiety, depression, hostility, fatigue and confusion (48–50). It was shown in *in vivo* and *in vitro* models that exposure to stress hormones, such as glucocorticoids or catecholamines, enhanced DNA damage, decreased the DNA repair capacity and suppressed *Trp53* levels (51, 52).

The second assumption can be achieved by the decreased elimination of damaged cells in mice concomitantly receiving CRIPS and Fe-TBI. Because of their structural abnormality with two or no centromeres, DCs and AFs are impaired in chromosome segregation and lost frequently with cell division. Thus, they are called unstable-type CAs. On the other hand, translocations and insertions keep their monocentric chromosomal structure and are believed not to be impaired in chromosome segregation. Thus, they are called stable-type CAs. It is known, however, that some fractions of stable-type CAs induced not only by high-LET radiation but also by high-dose, low-LET radiation degraded over time (53–56). Translocations induced in mouse splenocytes (female Swiss mouse, irradiated at 8 weeks of age) or peripheral blood cells (C57BL/6, female, irradiated at 8 weeks of age) after total-body X-ray or g-ray irradiation at not less than 2 Gy appeared to be degraded over time at least within the first 3–4 months of after TBI (53–55). Translocations induced in peripheral blood cells by 1 Gy Fe-TBI declined in frequency in a manner reminiscent

TABLE 1
Number of Chromosomal Aberrations in Mouse Splenocytes Subjected to CRIPS and/or Fe-TBI

| Exp. group, mouse ID | No. metaphase cells | No. abnormal cells (%) | No. CJs (/100 CEQ ^a) | FISH analysis by PAINT system | | |
|-------------------------|------------------------|---------------------------|-------------------------------------|--|--|---|
| | | | | No. translocations (/100 CEQ ^a) | Stable-type CAs | |
| | | | | | No. insertions (/100 CEQ ^a) | No. stable- type CAs (/100 CEQ ^a) |
| Free, 0.0 Gy | | | | | | |
| F00_1 | 449 | 1 (0.22) | 0 (0.00) | 0 (0.00) | 0 (0.00) | 0 (0.00) |
| F00_2 | 457 | 0 (0.00) | 0 (0.00) | 0 (0.00) | 0 (0.00) | 0 (0.00) |
| F00_3 | 511 | 1 (0.20) | 2 (1.19) | 0 (0.00) | 0 (0.00) | 0 (0.00) |
| F00_4 | 457 | 0 (0.00) | 0 (0.00) | 0 (0.00) | 0 (0.00) | 0 (0.00) |
| F00_5 | 453 | 1 (0.22) | 0 (0.00) | 0 (0.00) | 0 (0.00) | 0 (0.00) |
| F00_6 | 464 | 0 (0.00) | 0 (0.00) | 0 (0.00) | 0 (0.00) | 0 (0.00) |
| Total | 2,791 | 3 | 2 | 0 | 0 | 0 |
| (Average ± SE) | (465) | (0.11 ± 0.12) | (0.20 ± 0.48) | (0.00 ± 0.00) | (0.00 ± 0.00) | (0.00 ± 0.00) |
| Free, 0.1 Gy | | | | | | |
| F01_1 | 471 | 1 (0.21) | 0 (0.00) | 0 (0.00) | 0 (0.00) | 0 (0.00) |
| F01_2 | 473 | 1 (0.21) | 0 (0.00) | 0 (0.00) | 0 (0.00) | 0 (0.00) |
| F01_3 | 458 | 1 (0.22) | 0 (0.00) | 0 (0.00) | 0 (0.00) | 0 (0.00) |
| F01_4 | 448 | 1 (0.22) | 0 (0.00) | 0 (0.00) | 0 (0.00) | 0 (0.00) |
| F01_5 | 487 | 1 (0.21) | 2 (1.24) | 2 (1.24) | 0 (0.00) | 2 (1.24) |
| F01_6 | 485 | 2 (0.41) | 0 (0.00) | 0 (0.00) | 0 (0.00) | 0 (0.00) |
| Total | 2,822 | 7 | 2 | 2 | 0 | 2 |
| (Average ± SE) | (470) | (0.25 ± 0.08) | (0.21 ± 0.51) | (0.21 ± 0.51) | (0.00 ± 0.00) | (0.21 ± 0.51) |
| Free, 2.0 Gy | | | | | | |
| F20_1 | 212 | 11 (5.19) | 24 (34.3) | 13 (18.6) | 2 (2.86) | 15 (21.4) |
| F20_2 | 206 | 12 (5.83) | 13 (19.1) | 12 (17.7) | 0 (0.00) | 12 (17.7) |
| F20_3 | 208 | 7 (3.37) | 7 (10.2) | 4 (5.83) | 0 (0.00) | 4 (5.83) |
| F20_4 | 206 | 11 (5.34) | 28 (41.2) | 14 (20.6) | 4 (5.88) | 18 (26.5) |
| F20_5 | 204 | 5 (2.45) | 10 (14.9) | 7 (10.4) | 0 (0.00) | 7 (10.4) |
| F20_6 | 210 | 11 (5.24) | 15 (21.6) | 10 (14.4) | 1 (1.44) | 11 (15.9) |
| Total | 1,246 | 57 | 97 | 60 | 7 | 67 |
| (Average ± SE) | (208) | (4.57 ± 1.34) | (23.6 ± 11.9) | (14.6 ± 5.58) | (1.70 ± 2.35) | (16.3 ± 7.44) |
| Restraint, 0.0 Gy | | | | | | |
| R00_1 | 479 | 2 (0.42) | 0 (0.00) | 0 (0.00) | 0 (0.00) | 0 (0.00) |
| R00_2 | 462 | 1 (0.22) | 2 (1.31) | 2 (1.31) | 0 (0.00) | 2 (1.31) |
| R00_3 | 469 | 1 (0.21) | 1 (0.65) | 0 (0.00) | 0 (0.00) | 0 (0.00) |
| R00_4 | 463 | 1 (0.22) | 0 (0.00) | 0 (0.00) | 0 (0.00) | 0 (0.00) |
| R00_5 | 456 | 0 (0.00) | 0 (0.00) | 0 (0.00) | 0 (0.00) | 0 (0.00) |
| R00_6 | 465 | 0 (0.00) | 0 (0.00) | 0 (0.00) | 0 (0.00) | 0 (0.00) |
| Total | 2,794 | 5 | 3 | 2 | 0 | 2 |
| (Average ± SE) | (466) | (0.18 ± 0.16) | (0.33 ± 0.55) | (0.22 ± 0.54) | (0.00 ± 0.00) | (0.22 ± 0.54) |
| Restraint, 0.1 Gy | | | | | | |
| R01_1 | 490 | 0 (0.00) | 0 (0.00) | 0 (0.00) | 0 (0.00) | 0 (0.00) |
| R01_2 | 491 | 2 (0.41) | 2 (1.23) | 0 (0.00) | 0 (0.00) | 0 (0.00) |
| R01_3 | 466 | 3 (0.64) | 4 (2.60) | 4 (2.60) | 0 (0.00) | 4 (2.60) |
| R01_4 | 458 | 2 (0.44) | 2 (1.32) | 0 (0.00) | 0 (0.00) | 0 (0.00) |
| R01_5 | 439 | 1 (0.23) | 2 (1.38) | 0 (0.00) | 1 (0.69) | 1 (0.69) |
| R01_6 | 422 | 1 (0.24) | 2 (1.44) | 2 (1.44) | 0 (0.00) | 2 (1.44) |
| R01_7 | 467 | 1 (0.21) | 3 (1.95) | 1 (0.65) | 0 (0.00) | 1 (0.65) |
| Total | 3,233 | 10 | 15 | 7 | 1 | 8 |
| (Average ± SE) | (462) | (0.31 ± 0.21) | (1.42 ± 0.79) | (0.67 ± 1.01) | (0.10 ± 0.26) | (0.77 ± 0.97) |
| Restraint, 2.0 Gy | | | | | | |
| R20_1 | 226 | 11 (4.87) | 17 (22.8) | 10 (13.4) | 1 (1.34) | 11 (14.7) |
| R20_2 | 206 | 4 (1.94) | 4 (5.88) | 4 (5.88) | 0 (0.00) | 4 (5.88) |
| R20_3 | 208 | 12 (5.77) | 13 (18.9) | 5 (7.28) | 0 (0.00) | 5 (7.28) |
| R20_4 | 201 | 5 (2.49) | 9 (13.6) | 5 (7.54) | 1 (1.51) | 6 (9.05) |
| R20_5 | 210 | 15 (7.14) | 29 (41.8) | 16 (23.1) | 3 (4.33) | 19 (27.4) |
| R20_6 | 201 | 12 (5.97) | 21 (31.7) | 18 (27.1) | 0 (0.00) | 18 (27.1) |
| R20_7 | 202 | 8 (3.96) | 13 (19.5) | 7 (10.5) | 3 (4.50) | 10 (15.0) |
| Total | 1,454 | 67 | 106 | 65 | 8 | 73 |
| (Average ± SE) | (208) | (4.59 ± 1.90) | (22.0 ± 11.8) | (13.6 ± 8.36) | (1.67 ± 1.98) | (15.2 ± 8.94) |

^a CEQ = cell equivalent: Where an estimated number of chromosomal aberrations (CAs) occurred in a whole genome of 100 CEQs is shown.

^b Translocations, dicentrics (DCs) and acentric fragments (AFs) containing two or more color junctions (CJs) and simple insertions with two CJs were scored here. No insertions with three or more CJs were found.

^c Whole DCs were scored on the basis of the bright staining of centromeric heterochromatin with DAPI and include DCs scored by PAINT system as well.

TABLE 1
Extended.

| FISH analysis by PAINT system | | | | |
|-------------------------------------|-------------------------------------|---|---|--|
| Unstable-type CAs | | | | |
| No. DCs (/100 CEQ ^a) | No. AFs (/100 CEQ ^a) | No. unstable-type CAs (/100 CEQ ^a) | No. aberrant chromosomes with multiple CJs ^b (/100 CEQ ^a) | No. whole DCs ^c (/100 cells) |
| Free, 0.0 Gy | | | | |
| 0 (0.00) | 1 (0.67) | 1 (0.67) | 0 (0.00) | 0 (0.00) |
| 0 (0.00) | 0 (0.00) | 0 (0.00) | 0 (0.00) | 0 (0.00) |
| 1 (0.59) | 1 (0.59) | 2 (1.19) | 0 (0.00) | 1 (0.20) |
| 0 (0.00) | 0 (0.00) | 0 (0.00) | 0 (0.00) | 0 (0.00) |
| 0 (0.00) | 1 (0.67) | 1 (0.67) | 0 (0.00) | 0 (0.00) |
| 0 (0.00) | 0 (0.00) | 0 (0.00) | 0 (0.00) | 0 (0.00) |
| 1 | 3 | 4 | 0 | 1 |
| 0.10 ± 0.24 | 0.32 ± 0.35 | (0.42 ± 0.50) | (0.00 ± 0.00) | (0.03 ± 0.08) |
| Free, 0.1 Gy | | | | |
| 0 (0.00) | 1 (0.64) | 1 (0.64) | 0 (0.00) | 0 (0.00) |
| 0 (0.00) | 1 (0.64) | 1 (0.64) | 0 (0.00) | 0 (0.00) |
| 0 (0.00) | 0 (0.00) | 0 (0.00) | 0 (0.00) | 1 (0.22) |
| 0 (0.00) | 0 (0.00) | 0 (0.00) | 0 (0.00) | 1 (0.22) |
| 0 (0.00) | 0 (0.00) | 0 (0.00) | 0 (0.00) | 0 (0.00) |
| 0 (0.00) | 0 (0.00) | 0 (0.00) | 0 (0.00) | 2 (0.41) |
| 0 | 2 | 2 | 0 | 4 |
| (0.00 ± 0.00) | (0.21 ± 0.33) | (0.21 ± 0.33) | (0.00 ± 0.00) | (0.14 ± 0.17) |
| Free, 2.0 Gy | | | | |
| 1 (1.43) | 7 (10.0) | 8 (11.4) | 3 (4.29) | 7 (3.30) |
| 0 (0.00) | 5 (7.36) | 5 (7.36) | 0 (0.00) | 9 (4.37) |
| 1 (1.46) | 2 (2.91) | 3 (4.37) | 1 (1.46) | 10 (4.81) |
| 3 (4.41) | 3 (4.41) | 6 (8.83) | 5 (7.36) | 10 (4.85) |
| 2 (2.97) | 2 (2.97) | 4 (5.94) | 0 (0.00) | 2 (0.98) |
| 2 (2.89) | 3 (4.33) | 5 (7.22) | 1 (1.44) | 4 (1.90) |
| 9 | 22 | 31 | 10 | 42 |
| (2.19 ± 1.55) | (5.33 ± 2.80) | (7.52 ± 2.43) | (2.42 ± 2.88) | (3.37 ± 1.62) |
| Restraint, 0.0 Gy | | | | |
| 0 (0.00) | 2 (1.27) | 2 (1.27) | 0 (0.00) | 0 (0.00) |
| 0 (0.00) | 0 (0.00) | 0 (0.00) | 0 (0.00) | 0 (0.00) |
| 1 (0.65) | 0 (0.00) | 1 (0.65) | 0 (0.00) | 1 (0.21) |
| 0 (0.00) | 1 (0.65) | 1 (0.65) | 0 (0.00) | 0 (0.00) |
| 0 (0.00) | 0 (0.00) | 0 (0.00) | 0 (0.00) | 0 (0.00) |
| 0 (0.00) | 0 (0.00) | 0 (0.00) | 0 (0.00) | 0 (0.00) |
| 1 | 3 | 4 | 0 | 1 |
| (0.11 ± 0.26) | (0.32 ± 0.53) | (0.43 ± 0.52) | (0.00 ± 0.00) | (0.04 ± 0.09) |
| Restraint, 0.1 Gy | | | | |
| 0 (0.00) | 0 (0.00) | 0 (0.00) | 0 (0.00) | 0 (0.00) |
| 1 (0.62) | 1 (0.62) | 2 (1.23) | 0 (0.00) | 4 (0.81) |
| 0 (0.00) | 0 (0.00) | 0 (0.00) | 0 (0.00) | 2 (0.43) |
| 1 (0.66) | 2 (1.32) | 3 (1.98) | 0 (0.00) | 1 (0.22) |
| 0 (0.00) | 0 (0.00) | 0 (0.00) | 1 (0.69) | 0 (0.00) |
| 0 (0.00) | 0 (0.00) | 0 (0.00) | 0 (0.00) | 0 (0.00) |
| 1 (0.65) | 0 (0.00) | 1 (0.65) | 1 (0.65) | 1 (0.21) |
| 3 | 3 | 6 | 2 | 8 |
| (0.28 ± 0.34) | (0.28 ± 0.52) | (0.55 ± 0.79) | (0.19 ± 0.33) | (0.24 ± 0.30) |
| Restraint, 2.0 Gy | | | | |
| 3 (4.02) | 2 (2.68) | 5 (6.70) | 1 (1.34) | 8 (3.54) |
| 0 (0.00) | 0 (0.00) | 0 (0.00) | 0 (0.00) | 2 (0.97) |
| 3 (4.37) | 5 (7.28) | 8 (11.7) | 2 (2.91) | 10 (4.81) |
| 0 (0.00) | 1 (1.51) | 1 (1.51) | 2 (3.02) | 4 (1.99) |
| 3 (4.33) | 8 (11.5) | 11 (15.9) | 3 (4.33) | 11 (5.24) |
| 2 (3.02) | 3 (4.52) | 5 (7.54) | 0 (0.00) | 10 (4.98) |
| 0 (0.00) | 3 (4.50) | 3 (4.50) | 3 (4.50) | 5 (2.48) |
| 11 | 22 | 33 | 11 | 50 |
| (2.25 ± 2.15) | (4.58 ± 3.87) | (6.83 ± 5.57) | (2.30 ± 1.89) | (3.43 ± 1.66) |

TABLE 2
Number of Aberrant Chromosomes with Color Junctions (CJs)

| | Translocations | Insertions | DCs | AFs | Total |
|-----------------------------------|----------------|-----------------|----------------|-----------------|-------|
| No. of chromosomes with 1 CJ | 134 | NA | 23 | 21 | 178 |
| No. of chromosomes with 2 CJs | 2 ^a | 16 ^b | 2 ^c | 2 ^d | 22 |
| No. of chromosomes with 3 CJs | 0 | 0 | 0 | 1 ^e | 1 |
| Total no. of chromosomes with CJs | 136 | 16 | 25 | 24 ^f | 201 |
| Total no. of CJs | 138 | 32 | 27 | 28 | 225 |

^a Both chromosomes belong to experimental group F20.

^b Seven chromosomes belong to F20, one to R01 and eight to R20.

^c One chromosome belongs to R01 and one to R20.

^d Both chromosomes belong to R20.

^e This chromosome belongs to F20.

^f A total of 55 AFs with FISH paintings were found. Of these, 24 involved CJs and 31 did not.

Abbreviations: DCs = dicentrics; AFs = acentric fragments.

of those induced by 3 Gy or 4 Gy γ rays (56). The decay of stable-type CAs is expected to be attributed to the loss of heavily damaged cells, i.e., cells with multiple and/complex aberrations. If a cell possesses DCs in addition to translocations, these translocations may be lost during cell division. Cells with multiple CAs may be induced more frequently at high doses than at low doses (53, 54) and more frequently by high-LET radiation than by low-LET radiation (57). It was also shown that high-LET radiation induces complex CAs more frequently than low-LET radiation (44, 45). Complex CAs were previously shown to be less stable than simple ones (53, 54).

We previously examined the effects of CRIPS and X-ray TBI on *Trp53*-wild-type mice using the same experimental setup and conditions as the current work, and found no induction of CAs by exposure to CRIPS alone (32). In the current work, we again found no induction of CAs by CRIPS alone in *Trp53*^{+/-} mice, while haploinsufficiency of the *Trp53* gene might make *Trp53*^{+/-} mice more sensitive to the induction of DNA damage by CRIPS than *Trp53*-wild-type mice. On the other hand, Fischman *et al.* analyzed rat psychological stress models induced by forced swims, exposure to white noise or inescapable electrical foot shock, and found induction of CAs as well as sister chromatid exchanges (SCEs) in bone marrow cells (47). In that work, bone marrow cells were harvested one day after the psychological stress-inducing treatments and observation of chromosomes was performed by the Giemsa staining-based method intended to detect SCEs. Although the type of CAs observed was not documented in their report, they should be of the unstable type, such as breaks, as the stable type, such as translocations, is hardly detectable by the Giemsa staining method optimized for SCEs. To our knowledge, to date, no work on induction of chromosomal exchanges in animal models of psychological stress is available in the literature. Since our analyses were mainly focused on chromosomal exchanges and only chromosomal breaks occurring in chromosomes 1, 2 and 3 were scored, and because chromosomal breaks can occur spontaneously at relatively high frequency in mock-treated control animals as well, it is possible that subtle increases in chromosomal

breaks induced by psychological stress have gone unnoticed in our work.

Rithidech *et al.* compared induction of chromosomal damages in bone marrow cells of CBA/CaJ mice at 7 days after TBI at various doses with Fe (1 GeV/u, 159.5 Kev/mm; 0, 0.1, 0.5 and 1.0 Gy) and γ rays (0, 0.5, 1.0 and 3.0 Gy) using the whole-genome multi-color FISH (mFISH) technique and found a dose-dependent increase of CAs by each type of radiation (58). Most (75%) of the CAs in 0.1 Gy Fe-TBI mice were chromatid-type breaks, and the remaining 25% were Robertsonian translocations. Other common translocations were observed after 0.5 or 1.0 Gy Fe-TBI but not after 0.1 Gy Fe-TBI. Based on the linear term of dose-response curves, they concluded that Fe-TBI was 4.2 times more effective at inducing chromosomal breaks than g-ray TBI, but only 1.6 times more effective at inducing all types of exchanges including Robertsonian translocations. As described above, our FISH analysis is focused on chromosomal exchanges and can detect only 33% of those occurring in whole genome. In addition, we did not score Robertsonian translocations because they represent different features from other common translocations (36, 37, 59). Furthermore, our observation took place at 3 weeks postirradiation. Cells bearing unstable-type aberrations such as chromosomal breaks should be removed with cell divisions, if they were present at day 7 postirradiation. These are the probable reasons that induction of CAs by 0.1 Gy Fe-TBI was not observed in the current study.

High-LET radiation from HZE particles exhibits a highly energetic and dense core of the HZE particle tracks and a laterally extending low-LET secondary radiation, termed δ rays. The average number of Fe particle tracks traversing the nucleus of splenocytes (cross-sectional area estimate of 100 μm^2) calculated from an LET of 200 KeV/ μm are 0.31 and 6.24 for doses of 0.1 and 2.0 Gy, respectively. Under the assumption of a Poisson distribution, the probabilities of a cell nucleus which would receive zero, one, two, three and more particles at 0.1 Gy Fe-TBI are 73.3%, 22.7%, 3.5%, 0.4% and 0.0%, respectively. The probabilities at 2.0 Gy are 0.2%, 1.2%, 3.8%, 7.9% and

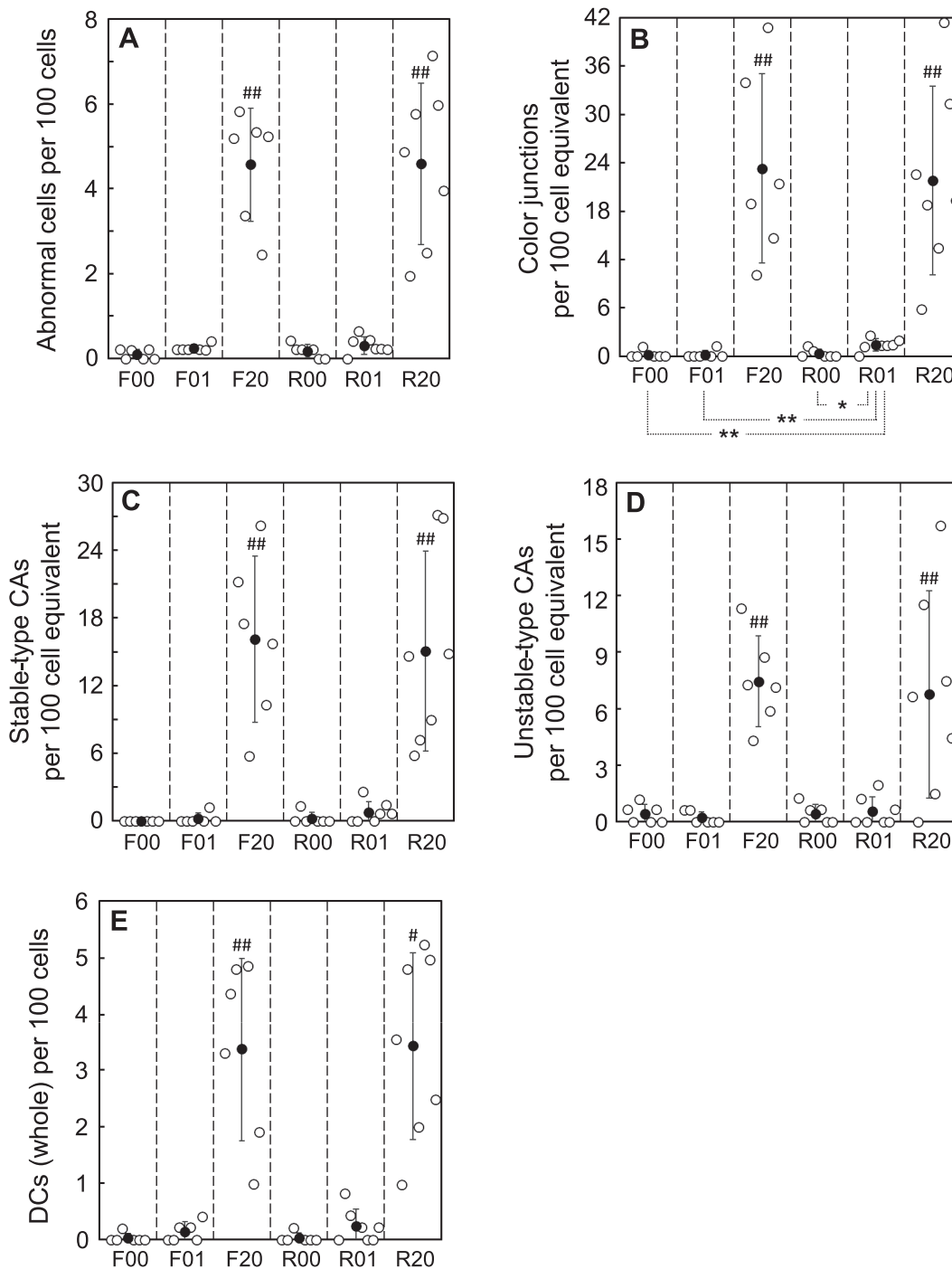


FIG. 4. Frequencies of aberrant chromosomes in splenocytes from mice subjected to CRIPS and/or Fe-TBI. Frequencies of abnormal cells (panel A), color junctions (panel B), stable-type CAs (panel C), unstable-type CAs (panel D) and whole DCs (panel E) are shown. Open circles indicate the values for individual mice and closed symbols with vertical bars indicate the mean numbers with standard deviations of each group: Free + 0.0 Gy (F00); free + 0.1 Gy (F01); free + 2.0 Gy (F20); restraint + 0.0 Gy (R00); restraint + 0.1 Gy (R01); and restraint + 2.0 Gy (R20). Statistically significant differences are indicated at * $P < 0.05$ and ** $P < 0.001$.

* $P < 0.001$ and ** $P < 0.05$, above the SD bars for F20 and R20 indicate significant differences of each group compared to F00, F01, R00 and R01 groups. For example, all P values (Student's t test) for comparisons between F20 and F00, F01, R00 or R01 were less than 0.01.

86.9%, respectively. In a previously published study on 1 GeV/u Fe particle radiation it was estimated that approximately 32 cells are hit by δ rays for each cell traversed by a primary Fe particle and that 19% of the energy is deposited

in cells that are hit only by the δ rays at low doses (60). Thus, it was postulated that, in 0.1 Gy Fe-TBI mice, 73.3% of cells were free from Fe particle tracks and some part of them received δ rays of 19 mGy and that 23% of cells were

traversed once by Fe particles and the remaining 4% cells received more than two particles. HZE particles yield complex chromosomal rearrangements at higher frequency than low-LET radiations even at low doses and complex-type exchanges frequently lead to cell death (61). In addition, most of the chromosomal exchanges we observed here in mice after Fe-TBI were simple-type, i.e., either reciprocal translocations or DCs with a paired AF. Taken together, it is likely that CAs found in splenocytes of *Trp53^{+/-}* mice that received both CRIPS and 0.1 Gy Fe-TBI resulted from δ rays but core of the Fe particle tracks. On the other hand, when mice received 2.0 Gy Fe-TBI, only 0.2% cells might be free from the particle tracks and 98.6% of cells might be traversed by the particle tracks multiple times. In addition, every cell might receive δ rays many times. Also, our chromosomal analysis found CAs in 4.57% of cells at 3 weeks after 2.0 Gy Fe-TBI (Table 1, F20). As in the current work, FISH probes could detect 33% of whole inter-chromosomal exchanges, nearly 14% ($4.57\% \times 3$) cells might have some CAs and 86% would be free from any CAs, even though 98.6% of cells were traversed multiple Fe particles. The observed frequency of CAs in the 2 Gy irradiated groups was much lower than the frequency calculated based on the hit number of Fe particle per cell. However, it is reasonable to expect that most of the splenocytes collected at end of the study were descendant cells of those mother cells that survived from the exposure, while most of the cells hit by multiple Fe particles should be severely damaged and die during 3 weeks after 2 Gy TBI.

Psychological stress as well as stress hormones (glucocorticoids and catecholamines) were found to decrease the levels and functions of *Trp53*, which plays a crucial role in the induction of growth arrest and/or apoptosis in damaged cells (31, 52). Feng *et al.* demonstrated reductions in *Trp53*-mediated apoptotic responses to radiation in the spleens of *Trp53^{+/+} C57BL/6J* mice exposed to CRIPS. Thus, CJs induced by 0.1 Gy Fe-TBI in our experiment might not be removed completely for 3 weeks after irradiation in *Trp53^{+/-}* mice with attenuated *Trp53*-mediated apoptotic and/or growth arrest responses resulting from concomitant exposure to CRIPS.

According to the estimation by NASA, assuming 10 g/cm² shielding and an ICRP 60 quality factor, exposure dose of spaceflight crews from cosmic rays during a future Mars mission at solar minimum should be 1.0–1.2 Sv (245–360 mGy) comprised of 50–80 mGy HZE particles, 45–70 mGy He, 130–180 mGy protons and 20–30 mGy neutrons and other particles (3). Using the *Trp53^{+/-}* mouse model, our current work demonstrates that Fe-TBI at 0.1 Gy can increase chromosomal exchanges in the presence of CRIPS, and that neither 0.1 Gy Fe-TBI nor CRIPS alone can do so. Fe-TBI at 0.1 Gy is comparable to the estimated dose of HZE particles to which spaceflight crews will be exposed during future Mars mission. Our findings suggest that psychological stress from challenging space environments may substantially enhance the genotoxic effects of HZE

particles derived from GCRs. Genotoxicity can cause cancer initiation. Psychological stress and resulting immune system weakening are major health concerns for spaceflight crews and may lead to promotion and progression of initiated cells (27, 28). Whether similar synergistic effects on CA induction could be induced in *Trp53^{+/+}* mice is unclear. Further analysis is required to clarify the cancer risks to spaceflight crews during future Mars mission.

ACKNOWLEDGMENTS

This work was partially supported by both the Ministry of Education, Culture, Sports, Science and Technology Grant-in-Aid for Scientific Research on Innovative Areas (grant nos. JP15K21745, 15H05944 and 15H05935 “Living in Space”) and three HIMAC Research Project Grants (nos. 22B258, 14J286 and 16J295).

We thank Ms. Hiromi Arai, Mr. Sadao Hirobe, Ms. Mikiko Nakajima, Ms. Chianing Hsieh and Ms. Yasuko Morimoto for their expert technical assistance and administrative support. We also thank Dr. Hideo Tsuji, Dr. Yoshihisa Kubota, Dr. Taiki Kawagoshi and Ms. Naoko Shiomi for their technical support and valuable discussion on chromosome analyses. We are grateful to Dr. Kazutaka Doi for his valuable advice on statistical analysis. We also express our appreciation for the anonymous peer reviewers for providing the constructive comments that strengthened the presentation of this work.

Received: September 11, 2020; accepted: March 26, 2021; published online: April 26, 2021

REFERENCES

1. Benton ER, Benton EV. Space radiation dosimetry in low-Earth orbit and beyond. *Nucl Instrum Methods Phys Res B* 2001; 184:255–94.
2. Durante M, Cucinotta FA. Physical basis of radiation protection in space travel. *Rev Mod Phys* 2011; 83:1245–81.
3. Nelson GA. Space radiation and human exposures, A primer. *Radiat Res* 2016; 185:349–58.
4. Sato T, Nagamatsu A, Ueno H, Kataoka R, Miyake S, Takeda K, et al. Comparison of cosmic-ray environments on earth, moon, mars and in spacecraft using PHITS. *Radiat Prot Dosimetry* 2018; 180:146–49.
5. Furukawa S, Nagamatsu A, Neno M, Fujimori A, Kakinuma S, Katsube T, et al. Space radiation biology for “Living in Space”. *Biomed Res Int* 2020; 2020:4703286.
6. Uri J. Space Station 20th: Long-duration missions. In: Mars K editor. *NASA History*. Washington, DC: National Aeronautics and Space Administration; 2020.
7. Bourdarie S, Xapsos M. The near-Earth space radiation environment. *IEEE Trans Nucl Sci* 2008; 55:1810–32.
8. Durante M, Cucinotta FA. Heavy ion carcinogenesis and human space exploration. *Nat Rev Cancer* 2008; 8:465–72.
9. Tobias CA, Lyman JT, Chatterjee A, Howard J, Maccabee HD, Raju MR, et al. Radiological physics characteristics of the extracted heavy ion beams of the bevatron. *Science* 1971; 174:1131–4.
10. Garrett-Bakelman FE, Darshi M, Green SJ, Gur RC, Lin L, Macias BR, et al. The NASA Twins Study: A multidimensional analysis of a year-long human spaceflight. *Science* 2019; 364:eaau8650.
11. Mars Architecture Steering Group. Human exploration of Mars: Design Reference Architecture 5.0. Report No. SP-2009-566. Houston: NASA Johnson Space Center; 2009. (<https://go.nasa.gov/3uoyT4k>)
12. Chida Y, Hamer M, Wardle J, Steptoe A. Do stress-related

- psychosocial factors contribute to cancer incidence and survival? *Nat Clin Pract Oncol* 2008; 5:466–75.
13. Trachtman JN. Post-traumatic stress disorder and vision. *Optometry* 2010; 81:240–52.
 14. Hyland ME, Alkhalaf AM, Whalley B. Beating and insulting children as a risk for adult cancer, cardiac disease and asthma. *J Behav Med* 2013; 36:632–40.
 15. Johansson L, Guo X, Hallstrom T, Norton MC, Waern M, Ostling S, et al. Common psychosocial stressors in middle-aged women related to longstanding distress and increased risk of Alzheimer's disease: a 38-year longitudinal population study. *BMJ Open* 2013; 3:e003142.
 16. Johnson SB, Riley AW, Granger DA, Riis J. The science of early life toxic stress for pediatric practice and advocacy. *Pediatrics* 2013; 131:319–27.
 17. Bergmann N, Gyntelberg F, Faber J. The appraisal of chronic stress and the development of the metabolic syndrome: a systematic review of prospective cohort studies. *Endocr Connect* 2014; 3:R55–80.
 18. von Bonsdorff MB, von Bonsdorff M, Kulmala J, Tormakangas T, Seitsamo J, Leino-Arjas P, et al. Job strain in the public sector and hospital in-patient care use in old age: a 28-year prospective follow-up. *Age Ageing* 2014; 43:393–9.
 19. Reiche EM, Nunes SO, Morimoto HK. Stress, depression, the immune system, and cancer. *Lancet Oncol* 2004; 5:617–25.
 20. Steptoe A, Kivimaki M. Stress and cardiovascular disease. *Nat Rev Cardiol* 2012; 9:360–70.
 21. Powell ND, Tarr AJ, Sheridan JF. Psychosocial stress and inflammation in cancer. *Brain Behav Immun* 2013; 30:S41–7.
 22. Wang B, Katsube T, Begum N, Neno M. Revisiting the health effects of psychological stress-its influence on susceptibility to ionizing radiation: a mini-review. *J Radiat Res* 2016; 57:325–35.
 23. Crucian BE, Zwart SR, Mehta S, Uchakin P, Quiarte HD, Pierson D, et al. Plasma cytokine concentrations indicate that in vivo hormonal regulation of immunity is altered during long-duration spaceflight. *J Interferon Cytokine Res* 2014; 34:778–86.
 24. Crucian B, Stowe RP, Mehta S, Quiarte H, Pierson D, Sams C. Alterations in adaptive immunity persist during long-duration spaceflight. *NPJ Microgravity* 2015; 1:15013.
 25. Bigley AB, Agha NH, Baker FL, Spielmann G, Kunz HE, Mylabathula PL, et al. NK cell function is impaired during long-duration spaceflight. *J Appl Physiol* (1985) 2019; 126:842–53.
 26. Buchheim JI, Matzel S, Rykova M, Vassilieva G, Ponomarev S, Nichiporuk I, et al. Stress related shift toward inflammaging in cosmonauts after long-duration space flight. *Front Physiol* 2019; 10:85.
 27. Makedonas G, Mehta S, Chouker A, Simpson RJ, Marshall G, Orange JS, et al. Specific immunologic countermeasure protocol for deep-space exploration missions. *Front Immunol* 2019; 10:2407.
 28. Crucian BE, Makedonas G, Sams CF, Pierson DL, Simpson R, Stowe RP, et al. Countermeasures-based improvements in stress, immune system dysregulation and latent herpesvirus reactivation onboard the International Space Station – Relevance for deep space missions and terrestrial medicine. *Neurosci Biobehav Rev* 2020; 115:68–76.
 29. Jenkins FJ, Van Houten B, Bovbjerg DH. Effects on DNA damage and/or repair processes as biological mechanisms linking psychological stress to cancer risk. *J Appl Biobehav Res* 2014; 19:3–23.
 30. Mukherjee D, Coates PJ, Lorimore SA, Wright EG. Responses to ionizing radiation mediated by inflammatory mechanisms. *J Pathol* 2014; 232:289–99.
 31. Feng Z, Liu L, Zhang C, Zheng T, Wang J, Lin M, et al. Chronic restraint stress attenuates p53 function and promotes tumorigenesis. *Proc Natl Acad Sci U S A* 2012; 109:7013–8.
 32. Katsube T, Wang B, Tanaka K, Ninomiya Y, Vares G, Kawagoshi T, et al. Effects of chronic restraint-induced stress on radiation-induced chromosomal aberrations in mouse splenocytes. *Mutat Res* 2017; 813:18–26.
 33. Tsukada T, Tomooka Y, Takai S, Ueda Y, Nishikawa S, Yagi T, et al. Enhanced proliferative potential in culture of cells from p53-deficient mice. *Oncogene* 1993; 8:3313–22.
 34. Wang B, Tanaka K, Katsube T, Ninomiya Y, Vares G, Liu Q, et al. Chronic restraint-induced stress has little modifying effect on radiation hematopoietic toxicity in mice. *J Radiat Res* 2015; 56:760–7.
 35. Tucker JD, Morgan WF, Awa AA, Bauchinger M, Blakey D, Cornforth MN, et al. A proposed system for scoring structural aberrations detected by chromosome painting. *Cytogenet Cell Genet* 1995; 68:211–21.
 36. Cazaux B, Catalan J, Claude J, Britton-Davidian J. Non-random occurrence of Robertsonian translocations in the house mouse (*Mus musculus domesticus*): is it related to quantitative variation in the minor satellite? *Cytogenet Genome Res* 2014; 144:124–30.
 37. Garagna S, Page J, Fernandez-Donoso R, Zuccotti M, Searle JB. The Robertsonian phenomenon in the house mouse: mutation, meiosis and speciation. *Chromosoma* 2014; 123:529–44.
 38. Kawagoshi T, Shiomi N, Takahashi H, Watanabe Y, Fuma S, Doi K, et al. Chromosomal aberrations in large Japanese field mice (*Apodemus speciosus*) captured near Fukushima Dai-ichi Nuclear Power Plant. *Environ Sci Technol* 2017; 51:4632–41.
 39. Guéguinou N, Huin-Schohn C, Bascove M, Bueb JL, Tschirhart E, Legrand-Frossi C, et al. Could spaceflight-associated immune system weakening preclude the expansion of human presence beyond Earth's orbit? *J Leukoc Biol* 2009; 86:1027–38.
 40. Kanas N, Sandal G, Boyd J, Gushin V, Manzey D, North R, et al. Psychology and culture during long-duration space missions. *Acta Astronautica* 2009; 64:659–77.
 41. Gridley DS, Pecaut MJ, Nelson GA. Total-body irradiation with high-LET particles: acute and chronic effects on the immune system. *Am J Physiol Regul Integr Comp Physiol* 2002; 282:R677–88.
 42. Gridley DS, Pecaut MJ. Genetic background and lymphocyte populations after total-body exposure to iron ion radiation. *Int J Radiat Biol* 2011; 87:8–23.
 43. Datta K, Suman S, Trani D, Doiron K, Rotolo JA, Kallakury BV, et al. Accelerated hematopoietic toxicity by high energy (56)Fe radiation. *Int J Radiat Biol* 2012; 88:213–22.
 44. Lee R, Sommer S, Hartel C, Nasonova E, Durante M, Ritter S. Complex exchanges are responsible for the increased effectiveness of C-ions compared to X-rays at the first post-irradiation mitosis. *Mutat Res* 2010; 701:52–9.
 45. Berardinelli F, De Vitis M, Nieri D, Cherubini R, De Nadal V, Gerardi S, et al. mBAND and mFISH analysis of chromosomal aberrations and breakpoint distribution in chromosome 1 of AG01522 human fibroblasts that were exposed to radiation of different qualities. *Mutat Res Genet Toxicol Environ Mutagen* 2015; 793:55–63.
 46. Adachi S, Kawamura K, Takemoto K. Oxidative damage of nuclear DNA in liver of rats exposed to psychological stress. *Cancer Res* 1993; 53:4153–5.
 47. Fischman HK, Pero RW, Kelly DD. Psychogenic stress induces chromosomal and DNA damage. *Int J Neurosci* 1996; 84:219–27.
 48. Kihara H, Teshima H, Sogawa H, Nakagawa T. Stress and superoxide production by human neutrophils. *Ann N Y Acad Sci* 1992; 650:307–10.
 49. Irie M, Asami S, Nagata S, Ikeda M, Miyata M, Kasai H. Psychosocial factors as a potential trigger of oxidative DNA damage in human leukocytes. *Jpn J Cancer Res* 2001; 92:367–76.
 50. Carroll JE, Marsland AL, Jenkins F, Baum A, Muldoon MF, Manuck SB. A urinary marker of oxidative stress covaries positively with hostility among midlife community volunteers. *Psychosom Med* 2010; 72:273–80.
 51. Flint MS, Baum A, Chambers WH, Jenkins FJ. Induction of DNA

- damage, alteration of DNA repair and transcriptional activation by stress hormones. *Psychoneuroendocrinology* 2007; 32:470–9.
52. Hara MR, Kovacs JJ, Whalen EJ, Rajagopal S, Strachan RT, Grant W, et al. A stress response pathway regulates DNA damage through beta2-adrenoreceptors and beta-arrestin-1. *Nature* 2011; 477:349–53.
 53. Hande MP, Boei JJ, Granath F, Natarajan AT. Induction and persistence of cytogenetic damage in mouse splenocytes following whole-body X-irradiation analysed by fluorescence in situ hybridization. I. Dicentrics and translocations. *Int J Radiat Biol* 1996; 69:437–46.
 54. Hande MP, Natarajan AT. Induction and persistence of cytogenetic damage in mouse splenocytes following whole-body X-irradiation analysed by fluorescence in situ hybridization. IV. Dose response. *Int J Radiat Biol* 1998; 74:441–8.
 55. Spruill MD, Nelson DO, Ramsey MJ, Nath J, Tucker JD. Lifetime persistence and clonality of chromosome aberrations in the peripheral blood of mice acutely exposed to ionizing radiation. *Radiat Res* 2000; 153:110–21.
 56. Tucker JD, Marples B, Ramsey MJ, Lutze-Mann LH. Persistence of chromosome aberrations in mice acutely exposed to $^{56}\text{Fe}^{+26}$ ions. *Radiat Res* 2004; 161:648–55.
 57. Durante M, George K, Wu H, Cucinotta FA. Karyotypes of human lymphocytes exposed to high-energy iron ions. *Radiat Res* 2002; 158:581–90.
 58. Rithidech KN, Honikel L, Whorton EB. mFISH analysis of chromosomal damage in bone marrow cells collected from CBA/CaJ mice following whole body exposure to heavy ions (^{56}Fe ions). *Radiat Environ Biophys* 2007; 46:137–45.
 59. Durante M, Gialanella G, Grossi GF, Nappo M, Pugliese M. The induction of Robertsonian translocations by X-rays and mitomycin C in mouse cells. *Mutat Res* 1994; 323:189–96.
 60. Brooks A, Bao S, Rithidech K, Couch LA, Braby LA. Relative effectiveness of HZE iron-56 particles for the induction of cytogenetic damage in vivo. *Radiat Res* 2001; 155:353–9.
 61. Ritter S, Durante M. Heavy-ion induced chromosomal aberrations: a review. *Mutat Res* 2010; 701:38–46.